Proc. Natl. Acad. Sci. USA
Vol. 90, pp. 6310–6314, July 1993
Biochemistry

DNA target selectivity by the vitamin D_3 receptor: Mechanism of dimer binding to an asymmetric repeat element

TERRI L. TOWERS*, BEN F. LUISI†, ALEXANDER ASIANOV*, AND LEONARD P. FREEDMAN*‡

*Cell Biology and Genetics Program, Memorial Sloan–Kettering Cancer Center, 1275 York Avenue, New York, NY 10021; and †Medical Research Council Virology Unit, Church Street, Glasgow G11 5JR, United Kingdom

Communicated by Paul B. Sigler, April 14, 1993

ABSTRACT **The 1,25-dihydroxyvitamin D_3 receptor, like other members of the nuclear receptor superfamily, forms dimers in solution that are probably stabilized by a dyad symmetrical interface formed by the ligand-binding domain. This receptor, however, recognizes DNA targets that are not dyad symmetric but rather are organized as direct repeats of a hexameric sequence with a characteristic 3-bp spacing. Using molecular modeling and site-directed mutagenesis, we have identified regions within the vitamin D_3 receptor zinc finger region that confer selectivity for direct repeats with appropriate spacing. Reflecting the organization of the DNA target, these regions, mapping to the tip of the first zinc finger module and the N and C termini of the second finger module, direct asymmetrical protein–protein contacts. A stereochemical model is proposed for these interactions.**

The human 1,25-dihydroxyvitamin D_3 receptor (hVDR) is a member of a superfamily of ligand-inducible transcription factors, which include the steroid and nuclear receptors. These proteins are characterized by a modular organization in which particular functions, such as ligand and DNA binding, are encompassed by discrete domains. The well-conserved DNA-binding domain contains two Zn finger-like modules (1–4), and this segment directs DNA sequence specificity through base contacts made by residues in the α-helix of module 1 (Fig. 1). In the case of the steroid receptors, such as the glucocorticoid and estrogen receptors, the domain also directs preference for palindromic targets through a self-complementary interface made by residues in module 2 (4), a region referred to as the D-box (6). As a result of protein–protein interactions formed by the optimal alignment of the dimerization interface, two molecules of the DNA-binding domain of the steroid receptors bind their targets cooperatively (7–10).

In contrast to the palindromic symmetry of the steroid receptor response elements, the DNA targets for hVDR and many other nuclear receptors are often organized as direct repeats (DRs). Although the half-site sequence of various nuclear receptor response elements is frequently the same, the spacing between the sites differs and in some cases may give rise to target discrimination. Characteristic spacings can lead to activation *in vivo* of reporter genes by vitamin D_3, thyroid hormone receptor (TR), and retinoic acid receptors (RARs) (11, 12). All three receptors have also been shown to form heterodimers with the receptor for 9-*cis*-retinoic acid (13), called RXR (retinoid X receptor) (14); this association affects binding affinity and may result in a physiological interplay of the corresponding hormones (15–24).

hVDR recognizes a hexameric DNA sequence arranged as a DR with a spacing of 3 bp (DR+3) (11). We find that the hVDR DNA-binding domain (VDRdbd) binds a DR+3 target cooperatively, and we present evidence that this effect is mediated by protein–protein contacts. The protein monomers are proposed to lie in a head-to-tail orientation on the DNA so that the protein–protein contacts are nonequivalent. This type of interaction differs from that found in the steroid receptors, where dyad-symmetric contacts are made between monomers on palindromic DNA targets. Three possible regions within the VDRdbd that harbor the nonequivalent contacts were identified by modeling, using the crystal structure of the dimeric glucocorticoid receptor DNA-binding domain (GRdbd) bound to a glucocorticoid response element (4). Residues in these three regions were exchanged for the corresponding amino acids from the RAR and/or TR, and the DNA-binding patterns of these mutant proteins were tested with DR elements having spacers of 3, 4, and 5 bp. The mutants no longer bind the DR+3 element cooperatively. When the same substitutions are introduced into the full-length hVDR, the protein loses its preference to bind the DR+3 target over DR+4 and DR+5 targets. These observations suggest that an asymmetrical protein–protein interface is formed by the DNA-binding domain and is a critical component of hVDR's target recognition.

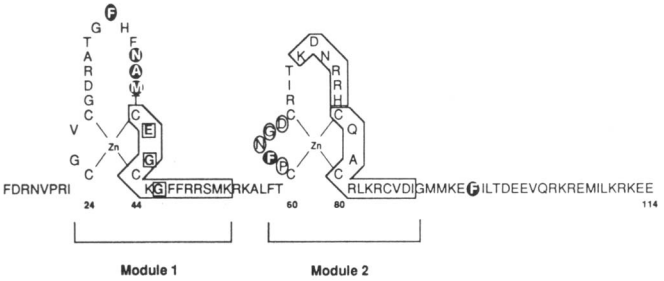

FIG. 1. Primary sequence and secondary structures of VDRdbd (5). Structural assignments are based on the crystal structure of the GRdbd–glucocorticoid response element complex (4). Helical regions are boxed. Residues in GRdbd that direct dyad symmetrical dimerization are circled; those residues shown to be important in target-site discrimination are boxed. Residues that are proposed here to form an asymmetric dimerization interface are circled and darkened.

MATERIALS AND METHODS

Construction of Bacterial Overexpression Vectors and Protein Purification. A vector for bacterial overexpression of full-length hVDR protein was constructed by modification of both ends of a hVDR cDNA clone (5) to create *Sma* I, *Eco*RI, *Bam*HI, and *Nde* I restriction sites at the 5′ end and *Hin*dIII and *Bam*HI sites at the 3′ end. This was accomplished by designing two oligonucleotides containing these sites and

The publication costs of this article were defrayed in part by page charge payment. This article must therefore be hereby marked "*advertisement*" in accordance with 18 U.S.C. §1734 solely to indicate this fact.

Abbreviations: hVDR, human vitamin D_3 receptor; VDRdbd, hVDR DNA-binding domain; GRdbd, glucocorticoid receptor DNA-binding domain; DR, direct repeat; RAR, retinoic acid receptor; RXR, retinoid X receptor; TR, thyroid hormone receptor.

‡To whom reprint requests should be addressed.

incorporating them into the hVDR sequence by PCR amplification. The 5′ primer sequence is 5′-CCCGGGAATTCGGATCCAACATATGGAGGCAATGGCGGCCAGCACTTCCCTG-3′; the 3′ primer sequence is 5′-CCCGGGGGATCCAAGCTTAGGAGATCTCATTGCCAAACACTTCG-3′. The amplified product was purified, digested with *Nde* I and *Bam*HI, and ligated into those sites in the T7 overexpression vector pAR3040 and used to transform BL21(DE3)/pLysS (25). Typically, 1000 ml of logarithmically growing culture was induced for 3 hr with 0.5 mM isopropyl β-D-thiogalactopyranoside; the cells were collected, resuspended in 5 vol of protein lysis buffer 1 [50 mM Tris·HCl, pH 7.5/1 mM EDTA/10% (vol/vol) glycerol/500 mM NaCl/4 mM $CaCl_2$/40 mM $MgCl_2$/5 mM dithiothreitol/0.5 mM phenylmethylsulfonyl fluoride], and sonicated on ice for three 10-sec intervals. The lysate was then incubated with DNase I (50 μg/ml) and RNase A (10 μg/ml) for 20 min and then centrifuged at 10,800 × *g* for 10 min. The pellet was resuspended in 10 vol of buffer 2 (50 mM Tris·HCl, pH 7.5/0.5 mM EDTA/10% glycerol/50 mM NaCl/100 μM $ZnCl_2$/5 mM dithiothreitol/0.1% Triton X-100). The pellet was resuspended in buffer 2 (without detergent) containing 6 M guanidine hydrochloride and incubated overnight at 4°C. After centrifugation for 10 min at 10,800 × *g*, the supernatant containing the denatured hVDR protein was renatured by dialysis for 8 hr against buffer 3, with three changes. The dialyzate was centrifuged at 14,000 rpm for 10 min and the supernatant was applied to a Superose 12 HR 10/30 column (Pharmacia) equilibrated with buffer 3. The pooled hVDR eluant was 70–80% pure, as assessed by SDS/PAGE. Vectors expressing the VDRdbd (residues 16–114) and its mutant derivatives were constructed and the protein products were purified as described (26). VDRdbd contains 14 N-terminal and 14 C-terminal non-VDR amino acids originating from the cloning vector and linkers; the sequences are ASMTGGQQMGRGSP and MGELGFPGLEDPST, respectively.

Oligonucleotide-Directed Mutagenesis. Site-directed mutagenesis was carried out by subcloning the hVDR- or VDRdbd-encoding fragment into pBluescript KS− (Stratagene), generating single-stranded template, and synthesizing the mutant strand with respective mutagenic oligonucleotides. The resulting mutant pools were screened for the appropriate codon changes by dideoxynucleotide DNA sequencing. Mutants were subcloned back into the original T7 vector and reconfirmed by sequencing; mutant proteins were overexpressed and purified as described above for VDRdbd and hVDR.

DNA-Binding Assay. DNA binding was assessed by gel mobility-shift electrophoresis as described (26). The sequences of the probes used (top strand, half-site recognition elements underlined) are as follows: DR1/2′, 5′-AGCTTCGCAGTTCAAGGAAGCTAGAGCA-3′; DR+3′ probe, 5′-AGCTTCGCAGTTCAAGGAGTTCAGAGCG-3′; DR+4′, 5′-AGCTTCGCAGTTCACAGGAGTTCAGAGCG-3′; and DR+5′, 5′-AGCTTCGCAGTTCACCAGGAGTTCAGAGCG-3′.

Quantitation of DNA Binding. Individual bands from mobility-shift gels representing free and bound DNA elements were recorded on a phosphor screen for 30 min and scanned with a Phosphoimager 400-E (Molecular Dynamics) set to detect ^{32}P radioactive emissions; the signals were digitized and quantified with Image Quant software (Molecular Dynamics) and corrected for background. Cooperativity was determined by calculating the Hill's coefficient of both wild-type and mutant VDRdbd derivatives to the DR+3′ target probe. Hill's coefficient is the maximal slope of $\log[Y/(1-Y)]$ versus $\log[P]$ at half-maximal saturation, where Y is the fraction of sites occupied and $[P]$ is the protein concentration. A Hill's coefficient of 1.0 implies no cooperativity; >1.0 indicates positive cooperativity; <1.0 indicates negative cooperativity. The Hill's coefficients were calculated here by assuming two binding sites in the oligonucleotide probes.

RESULTS

hVDR Binds Preferentially to a DR+3 Element. Purified recombinant hVDR binds with high affinity to the vitamin D response element of the mouse osteopontin (*Spp-1*) gene (27). This target is composed of a DR of the half-site 5′-GGTTCA-3′ with a 3-bp separation. We designed a synthetic binding site that had equally high affinity for hVDR carrying a similar half site repeat 5′-AGTTCA-3′ (DR+3′; Fig. 2). Two half-sites appear to be required for strong hVDR binding, since the protein did not bind detectably to an element composed of a single half-site (Fig. 2). hVDR has an ≈30-fold lower affinity for sequences when the separation between the half-sites is increased by 1 or 2 bases (DR+4′ and DR+5′, respectively; Fig. 2). The purified hVDR binds the DNA target as a homodimer. Mixing hVDR with a larger glutathione-*S*-transferase–hVDR fusion protein results in three shifted species when bound to the DR+3′ target, suggesting that hVDR binds DNA as a dimer (data not shown). A similar result is seen when hVDR is mixed with a glutathione-*S*-transferase–RXRα fusion and bound to the target probe, confirming that hVDR also forms heterodimers with RXR on the DNA target. Like homodimeric hVDR, the heterodimer preferentially associates with the DR+3′ element over DR+4′ and DR+5′ (data not shown).

VDRdbd Alone Confers Half-Site Spacing Selectivity. The spacing preferences of hVDR were further examined by using the isolated DNA-binding domain (VDRdbd) (26). At low concentrations, a single shifted band is evident when this protein is incubated with a half-site element (DR1/2; Fig. 2 *Lower*) or with the DR+3′, DR+4′, and DR+5′ elements (shift 1 in Fig. 2), suggesting that VDRdbd, like the DNA-binding domains of the glucocorticoid and estrogen receptors, is monomeric in the absence of DNA (2, 3, 28). As the protein concentration is increased, a second VDRdbd monomer binds preferentially to the DR+3′ element (shift 2 in Fig. 2). Much higher levels are required for a second monomer to bind DR+4′ and DR+5′. Two VDRdbd monomers bind the DR+3′ cooperatively (i.e., binding of the first monomer favors binding of a second; see below and Fig. 3*C*) but bind DR+4′ and DR+5′ noncooperatively. This suggests that binding of the VDRdbd to a DR+3′ target could occur through favorable protein–protein interactions resulting from stereospecific alignment of a dimerization interface.

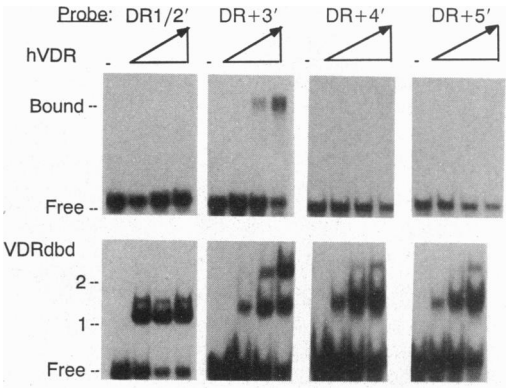

FIG. 2. Half-site spacing selectivity of hVDR and its DNA-binding domain. DNA-binding activities of overexpressed hVDR and VDRdbd proteins were assayed by gel-mobility retardation. In each panel, 0.5 ng of the indicated end-labeled probe was incubated with 0, 75, 150, and 300 ng of hVDR protein (*Upper*) or 0, 25, 50, and 100 ng of VDRdbd protein (*Lower*).

DNA-Binding Analysis of Asymmetric Dimer Interface Mutants. The interactions of two VDRdbd molecules on a direct repeat element were modeled using the crystal structure of the GRdbd–glucocorticoid response element complex (4). The model was constructed by rotating one of the GRdbd monomers by 180° in its binding site. The position of the rotated monomer in the major groove was fixed by base-specific contacts made by the N-terminal α-helix. Although this type of modeling cannot give accurate details of the interaction, it can reveal regions where contacts between monomers on a DR+3 element could be made. The modeling suggests that intermolecular contacts could form between residues in the vicinity of the C terminus of one monomer with residues in module 2 of the neighboring monomer (see Fig. 5). This interface may be supported by intramolecular contacts between residues in the tip of module 1 and residues in the vicinity of the C terminus of module 2 (regions of potential contact are highlighted in Fig. 1). The residues in these regions are hydrophobic, and the intramolecular packing would mask them from solvent.

We used site-directed mutagenesis to test the role of certain residues from the indicated regions in target site selection. As shown in Figs. 3 and 4, substitutions in the tip of module 1, the beginning of module 2, and the C-terminal boundary of module 2 all alter the spacing specificity of hVDR for a DR+3 element. The mutations replace hVDR residues with corresponding amino acids from TR and/or RAR, which preferentially bind to DR+4 and DR+5 sites, respectively. The single substitution F-34 → Y (F34Y) in the tip of the first finger results in hVDR binding equally well to DR+3′, DR+4′, and DR+5′ sites (see Fig. 4*A*). This relaxing of spacing specificity is also observed when the substitution F-62 → Y is introduced in the D-box of module 2 (Fig. 4*A*). The relaxation effect becomes more prominent when the two substitutions are introduced together (Fig. 3*A*) and may actually confer a modest preference for the DR+5′ element. Introducing this same double mutation into VDRdbd also alters its spacing selectivity: the mutant protein now exhibits the same titration behavior irrespective of half-site spacing (compare Fig. 3*B* and Fig. 2). Our results further indicate that while the wild-type VDRdbd occupies the two half-sites of a DR+3′ cooperatively, this cooperativity is abolished in the F34Y/F62Y double mutant (Fig. 3*C*). In Fig. 3*D*, these data are presented as Hill plots; the Hill coefficients for the wild-type and mutant proteins are 1.4 and 0.9, respectively. Importantly, the mutations do not appear to affect the affinity of the first DNA-bound monomer by more than a factor of 3. Therefore, the substitutions must disrupt favorable protein–protein interactions occurring when the monomers are aligned on the DR+3′ target.

The Role of the T-Box. An additional key region involved in the putative asymmetric interface is located just outside the C terminus of module 2 in a region referred to as the T-box for its role in RXRβ target recognition (30). We find that a substitution of F-93 of this box (Fig. 1) to alanine, the corresponding residue of RARγ, can relax hVDR binding site selectivity (Fig. 4*A*, lanes 28–36). This effect is qualitatively similar to that resulting from a single mutation of F-34 within module 1 or F-62 residing in the D-box of module 2 (lanes 10–18 and 19–27, respectively).

When the F93A mutation is combined with F34Y, the same loss of half-site spacing specificity is observed (data not shown), whereas the double-mutant F34Y/F62Y appears to gain a modest preference for the DR+5′ element (Fig. 3*A*). Intriguingly, this DR+5′ preference is further enhanced in a composite hVDR mutant carrying three additional mutations near the tip of module 1 (N37G/A38V/M39S) combined with changes at the three other positions already described (F-34, F-62, F-93) (Fig. 4*B*). Except for the F62Y substitution in the D-box, all the changes are to corresponding residues of the RARs, which prefer to bind to a DR+5 element. This multiple hVDR mutant heterodimerized with RXRα (as a glutathione-*S*-transferase–RXRα fusion) also exhibited a preference for the DR+5 site (data not shown).

Cumulatively, the results from the various mutants implicate three distinct but equally important segments of the VDRdbd as encoding the asymmetrical dimerization function: (*i*) the loop region of module 1; (*ii*) segments of module 2, including the previously defined D-box (6), a region that plays an important role in formation of the symmetrical dimer interface of steroid receptors (4); and (*iii*) the T-box, a region ≈5 residues beyond the C terminus of module 2 (Fig. 1).

DISCUSSION

The subgroup of nonsteroid receptors that recognize the estrogen response element core half-site, AGGTCA, may

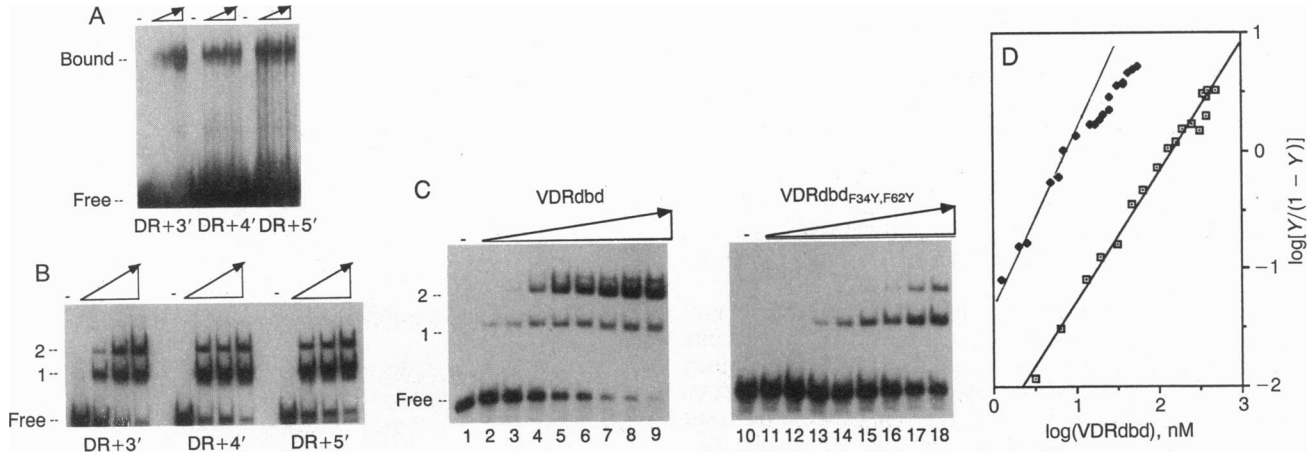

FIG. 3. Mutations in two regions of the DNA-binding domain relax spacing selectivity in hVDR. (*A*) Double-mutant F34Y/F62Y in hVDR abolishes preferences for DR+3′ over DR+4′ and DR+5′. Protein titrations were done as described in Fig. 2. (*B*) Double-mutant F34Y/F62Y in the context of the VDRdbd. Mutations weaken the preference for a dimer to bind DR+3′ over DR+4′ and DR+5′. (*C*) Cooperative binding of VDRdbd to a DR+3′ element (*Left*) and the loss of cooperativity in the double mutant (*Right*). Concentration of protein used in both titrations ranged from 7 to 280 nM. (*D*) Hill plots of the VDRdbd wild-type (◆) and mutant (⊡) DNA-binding titrations presented in *C*. Plots were obtained by using the logarithms of VDRdbd concentration (nM) and $Y/(1 - Y)$, where Y is the fraction of binding sites occupied. Slope becomes 0.8 at the higher end of the wild-type titration, whereas it should be 1.0 here as well as at the lower end (29), and the curve is asymmetric about the midpoint. These discrepancies may arise from gel artifacts.

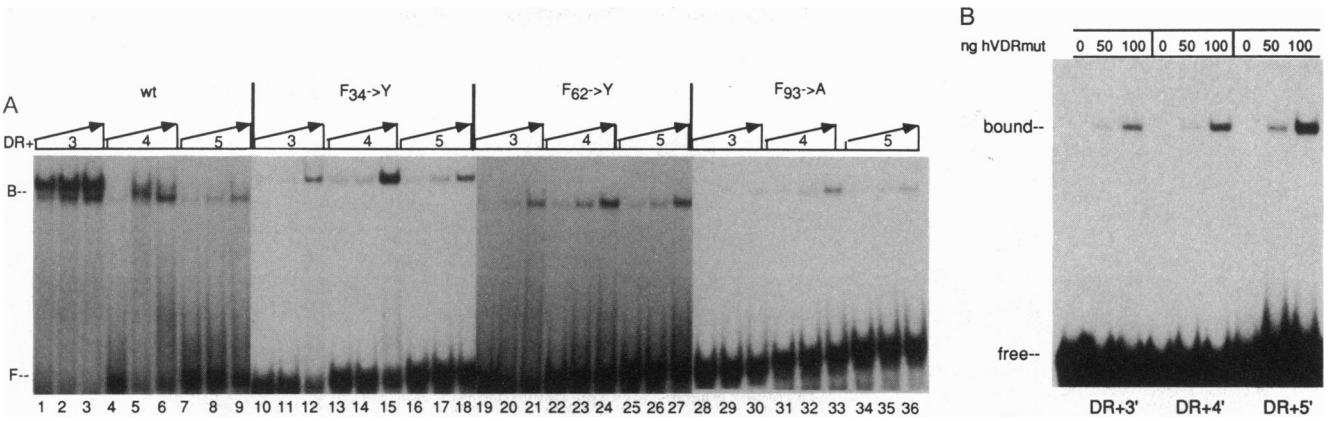

FIG. 4. (*A*) Single mutations are sufficient to relax hVDR spacing selectivity. In each series, 50, 100, and 200 ng of the indicated hVDR single-residue mutant was mixed with DR+3, DR+4, and DR+5 probes. Lanes: 1–9, wild-type (wt) hVDR; 10–18, hVDR F34Y; 19–27, hVDR F62Y; 28–36, hVDR F93A. F and B, free and bound probe, respectively. Note that mobilities of bound probe vary since wt hVDR and F62Y were electrophoresed on one gel, and F34Y/F93A were electrophoresed on another. (*B*) Composite mutant carrying substitutions in the three regions involved in an asymmetric interface relaxes the spacing selectivity. Mutations in hVDR (hVDRmut) are as follows: F34Y, N37G, A38V, M39S, F62Y, and F93A. For each probe, 0, 50, and 100 ng of the hVDR mutant was used, as indicated.

distinguish targets by recognizing the relative orientation and spacing of two such sites. This group includes TR, RAR, and VDR, as well as many orphan receptors. In some cases, the response elements are arranged as DRs, which suggests that the proteins may bind as asymmetrical dimers (i.e., in a head-to-tail orientation), in contrast to the steroid receptors, which form symmetrical dimers on their DNA targets. The asymmetrical dimer of hVDR, and perhaps other receptors, appears to be stabilized by protein–protein interactions within its DNA-binding domain, as we have described here.

Using a yeast genetic screen, Wilson *et al.* (30) have identified a region of RXRβ that confers transcriptional activation from an element composed of AGGTCA DRs with a single-base spacer. Amino acids mediating this effect lie in a region C-terminal to module 2, which they term the T-box. These investigators have suggested that residues in the T-box direct protein–protein interactions for RXRβ. We find that specific residues in the corresponding region of hVDR (i.e., F-93) play an analogous role and define in part the preference of hVDR for a DR+3 element.

We propose that the residues in the T-box region of hVDR make an intramolecular packing against residues in the tip of module 1 (Fig. 5*A*). For instance, the C-terminal residues F-93, I-94, and L-95 may make hydrophobic interactions with F-34 and with the residues N-37, A-38, and M-39 in module 1. This intramolecular interaction does not occur in the crystal structure of the GRdbd–DNA complex (4), where the corresponding residues are overall less hydrophobic. The proposed interaction would orient and stabilize the T-box of one hVDR monomer to make intermolecular contacts with module 2 of an adjacently bound monomer on the DR+3 element (Fig. 5*B*). For example, the charged and polar residues flanking the hydrophobic tripeptide (FIL) may contact charged residues in the short α-helix of module 2 (i.e., H-75) or within the D-box (Fig. 5*B*). The intramolecular hydrophobic interactions between the T-box and module 1, and the intermolecular contacts between the T-box and module 2, might be disrupted or diminished by the substitutions introduced here. The substitutions would therefore affect DNA-binding selectivity through effects on the asymmetrical dimerization interface. While the T-box region is poorly conserved in the nuclear receptor superfamily, there is a tendency for hydrophobic residues to cluster here and in the tip of module 1. The details of the interface may differ from receptor to receptor, but it is possible that other receptors might fold similarly to hVDR so that they too bind selectively to their respective targets through asymmetrical interactions of DNA-binding domains.

Recent experiments indicate that RXR forms heterodimers with many other nuclear receptors, including hVDR (15–21). The interaction of RXR with RAR and TR appears to be critical for recognition of certain direct repeat elements. For example, TR/RXR and RAR/RXR heterodimers bind preferentially to a DR+5 and a DR+4 element, respectively, whereas TR, RAR, and RXR alone do not (T. Perlmann and R. M. Evans, personal communication). In the case of hVDR, both the homodimer (as shown here) and the RXR–hVDR heterodimer bind preferentially to a DR+3 target. *In vivo*, there may be circumstances in which the homodimer is dominant and other conditions when the heterodimer is favored. Indeed, Carlberg *et al.* (32) have recently proposed a two-pathway system for vitamin D function that is controlled by homodimers and RXR heterodimers. This may result in complex physiological responses as a result of the interplay of the ligands and concentrations of the two receptors.

If full-length nuclear receptors were to associate with DNA in a fashion that mirrors the direct repeat, then these proteins might be expected to form virtually endless polymers. Instead, hVDR and other nuclear receptors form stable dimers: either homodimers or, in complex with RXR, heterodimers. This association probably occurs through a well-conserved interface made by the ligand-binding domain (33, 34), which probably has exact or approximate dyad symmetry for homodimers and heterodimers, respectively. The linkage between the interfaces made by the ligand-binding and DNA-binding domains must be sufficiently flexible to permit the latter domain to match the orientation of the sequence repeat of the DNA target site. The ligand-binding domain's dimer interface provides the principal organizational effect of bringing two DNA-reading heads within proximity of each other and would reduce the entropy penalty of association of the DNA-binding domain to its target. This interaction would in turn allow the proper interface between two DNA-binding domains to form and selectively match a direct or inverted repeat, depending on the interface (Fig. 5*C*).

As is the case with receptor sequence specificity, the spacing selectivity of hVDR and other steroid/nuclear receptors appears to be directed by a few amino acids at pivotal points in the DNA-binding domain. It seems a remarkable invention of evolution that small variations of this region have generated tremendous DNA-binding specificity and functional diversity in the superfamily.

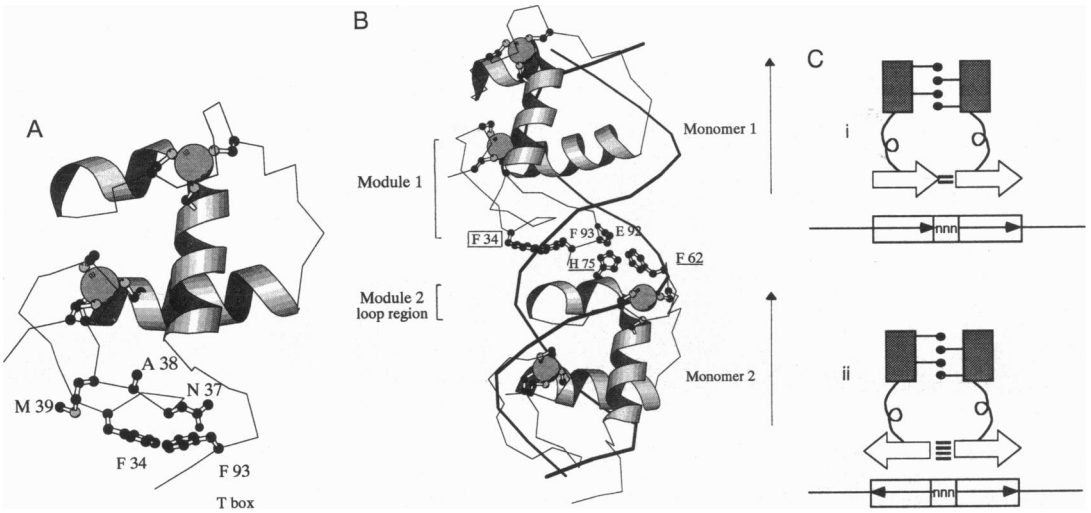

FIG. 5. Models for intramolecular and intermolecular contacts involved in asymmetric target-site binding. (*A*) Intramolecular interaction of the T-box of hVDR with the tip of module 1. Helices (ribbons), the C^{α} backbone trace (lines), side chains of selected residues of the T-box and module 1 tip (ball and stick), and metal coordinating cysteines are shown. The two zinc ions are represented by spheres. Recognition α-helix of module 1, which lies in the major groove of the DNA, is oriented horizontally. Principal helix of module 2 lies vertically. F-93 of the T-box may pack against N-37 and F-34, which is supported by A-38, and, possibly, M-39. I-94 and L-95 may also pack against the tip (not shown, for clarity). Hydrophobic interactions may orient the T-box to make intermolecular contacts, as suggested in *B*. (*B*) Orientation of monomers on the DNA. DNA in the background, and, for clarity, only a trace of its phosphate backbone is shown (thicker lines). Arrows on right indicate direction of sequence repeat and monomer orientation, which, for comparison, is the same as that of *A*. Brackets on left indicate approximate boundaries of module 1 from monomer 1 and the Zn loop region of module 2 from monomer 2. The module 1 residue, F-34, is boxed; all other indicated residues belong to module 2 (H-75 and F-62 from monomer 2, underlined) or the T-box (F-93 and E-92 from monomer 1). Intermolecular contacts could form between residues of the T-box (e.g., E-92) of one monomer and residues of the D-box and short α-helix in module 2 (such as H-75) of the neighboring monomer. *A* and *B* were prepared by using MOLSCRIPT (31). (*C*) Schematic showing relationship between target-site symmetry and protein–protein interactions. Case *i* illustrates dyad-symmetrical dimerization through the ligand-binding domain (shaded rectangles), which maintains the DNA-reading heads (open arrows) in proximity for association. The two domains are connected by a flexible peptide linker. Case *ii* shows the representative case of steroid receptors, where dyad-symmetric dimers bind elements composed of inverted repeats with suitable spacing.

We thank I. Alroy and M. Liu for help in preparing the figures; R. Benezra, F. Rastinejad, and K. Nagai for insightful comments on the manuscript; and R. M. Evans and T. Perlmann for communicating results prior to publication. This work was supported in part by a North Atlantic Treaty Organization Collaborative Research grant and by National Institutes of Health Grants DK45460-01 and NCI-P30-CA-08748.

1. Freedman, L. P., Luisi, B. F., Korszun, Z. R., Basavappa, R., Sigler, P. B. & Yamamoto, K. R. (1988) *Nature (London)* **334**, 543–546.
2. Hard, T., Kellenbach, E., Boelens, R., Maler, B. A., Dahlman, K., Freedman, L. P., Carlstedt-Duke, J., Gustafsson, J.-A., Yamamoto, K. R. & Kaptein, R. (1990) *Science* **249**, 157–160.
3. Schwabe, J. W. R., Neuhaus, D. & Rhodes, D. (1990) *Nature (London)* **348**, 458–461.
4. Luisi, B. F., Xu, W. X., Otwinowski, Z., Freedman, L. P., Yamamoto, K. R. & Sigler, P. B. (1991) *Nature (London)* **352**, 497–505.
5. Baker, A. R., McDonnel, D. P., Hughes, M., Crisp, T. M., Mangelsdorf, D. J., Haussler, M. R., Pike, J. W., Shine, J. & O'Malley, B. W. (1988) *Proc. Natl. Acad. Sci. USA* **85**, 3294–3298.
6. Umesono, K. & Evans, R. M. (1989) *Cell* **57**, 1139–1146.
7. Tsai, S. Y., Carstedt-Duke, J., Weigel, N. L., Dahlman, K., Gustafsson, J.-A., Tsai, M.-J. & O'Malley, B. W. (1988) *Cell* **55**, 361–369.
8. Dahlman-Wright, K., Wright, A., Gustafsson, J.-A. & Castedt-Duke, J. (1991) *J. Biol. Chem.* **266**, 3107–3112.
9. Hard, T., Dahlman, K., Carstedt-Duke, J., Gustafsson, J. A. & Rigler, R. (1990) *Biochemistry* **29**, 5358–5364.
10. Alroy, I. & Freedman, L. P. (1992) *Nucleic Acids Res.* **20**, 1045–1052.
11. Umesono, K., Murakami, K. K., Thompson, C. C. & Evans, R. M. (1991) *Cell* **65**, 1255–1266.
12. Naar, A. M., Boutin, J.-M., Lipkin, S. M., Yu, V. C., Holloway, J. M., Glass, C. K. & Rosenfeld, M. G. (1991) *Cell* **65**, 1267–1279.
13. Heyman, R. A., Mangelsdorf, D. J., Dyck, J. A., Stein, R. B., Eichele, G., Evans, R. M. & Thaller, C. (1992) *Cell* **68**, 397–406.
14. Mangelsdorf, D. J., Ong, E. S., Dyck, J. A. & Evans, R. M. (1990) *Nature (London)* **345**, 224–229.
15. Yu, V. C., Delsert, C., Andersen, B., Holloway, J. M., Devary, O. V., Naar, A. M., Kim, S. Y., Boutin, J. M., Glass, C. K. & Rosenfeld, M. G. (1991) *Cell* **67**, 1251–1266.
16. Zhang, X.-K., Hoffmann, B., Tran, P. B.-V., Graupner, G. & Pfahl, M. (1992) *Nature (London)* **355**, 441–446.
17. Kliewer, S. A., Umesono, K., Mangelsdorf, D. J. & Evans, R. M. (1992) *Nature (London)* **355**, 446–449.
18. Bugge, T. H., Pohl, J. O., Lonnoy, J. & Stunnenberg, H. (1992) *EMBO J.* **11**, 1409–1418.
19. Marks, M. S., Hallenbeck, P. L., Nagata, T., Segars, J. H., Appella, E., Nikodem, V. M. & Ozato, K. (1992) *EMBO J.* **11**, 1419–1435.
20. Leid, M., Kastner, P., Lyons, R., Nakshatri, H., Saunders, M., Zacharewski, T., Chen, J. A., Staub, A., Garnier, J. M., Mader, S. & Chambon, P. (1992) *Cell* **68**, 377–395.
21. Kliewer, S. A., Umesono, K., Noonan, D. J., Heyman, R. A. & Evans, R. M. (1992) *Nature (London)* **358**, 771–774.
22. deThe, H., Vivanco-ruiz, M., Tiollais, P., Stunnenberg, H. & Dejean, A. (1990) *Nature (London)* **343**, 177–180.
23. Sucov, H. M., Murakami, K. K. & Evans, R. M. (1990) *Proc. Natl. Acad. Sci. USA* **87**, 5392–5396.
24. Hoffmann, B., Lehmann, J. M., Zhang, X., Hermann, T., Husmann, M., Graupner, G. & Pfahl, M. (1990) *Mol. Endocrinol.* **4**, 1727–1736.
25. Studier, F. W. & Moffat, B. A. (1986) *J. Mol. Biol.* **189**, 113–130.
26. Freedman, L. P. & Towers, T. T. (1991) *Mol. Endocrinol.* **5**, 1815–1826.
27. Noda, M., Vogel, R. L., Craig, A. M., Prahl, J., DeLuca, H. F. & Denhardt, D. T. (1990) *Proc. Natl. Acad. Sci. USA* **87**, 9995–9999.
28. Freedman, L. P., Yamamoto, K. R., Luisi, B. F. & Sigler, P. J. (1988) *Cell* **54**, 444.
29. Cantor, C. R. & Schimmel, P. R. (1980) *Biophysical Chemistry* (Freeman, San Francisco), Part III, p. 861.
30. Wilson, T. E., Paulsen, R. E., Padgett, K. A. & Milbrant, J. (1992) *Science* **256**, 107–110.
31. Kraulis, P. J. (1991) *J. Appl. Crystallogr.* **24**, 946–954.
32. Carlberg, C., Bendik, I., Wyss, A., Meier, E., Sturzenbecker, L. J., Grippo, J. F. & Hunziker, W. (1993) *Nature (London)* **361**, 657–660.
33. Forman, B. M. & Samuels, H. H. (1990) *Mol. Endocrinol.* **4**, 1293–1301.
34. Farwell, S. E., Lees, J. A., White, R. & Parker, M. G. (1990) *Cell* **60**, 953–962.